Intrinsic mutant HTT-mediated defects in oligodendroglia cause myelination deficits and behavioral abnormalities in Huntington disease

Costanza Ferrari Bardile[a], Marta Garcia-Miralles[a], Nicholas S. Caron[b], Nirmala Arul Rayan[c], Sarah R. Langley[d,e], Nathan Harmston[d], Ana Maria Rondelli[f], Roy Tang Yi Teo[a], Sabine Waltl[b], Lisa M. Anderson[b], Han-Gyu Bae[g,h], Sangyong Jung[g,i], Anna Williams[f], Shyam Prabhakar[c], Enrico Petretto[d], Michael R. Hayden[a,b,j], and Mahmoud A. Pouladi[a,i,j,1]

[a]Translational Laboratory in Genetic Medicine, Agency for Science, Technology and Research (A*STAR), Immunos, 138648 Singapore; [b]Centre for Molecular Medicine and Therapeutics, BC Children's Hospital Research Institute, University of British Columbia, Vancouver BC V5Z 4H4, Canada; [c]Computational and Systems Biology, Genome Institute of Singapore, Agency for Science, Technology and Research (A*STAR), 138672 Singapore; [d]Centre for Computational Biology, Duke-NUS Medical School, 169857 Singapore; [e]Lee Kong Chian School of Medicine, Nanyang Technological University, 636921 Singapore; [f]The Medical Research Council Centre for Regenerative Medicine and Multiple Sclerosis Society Edinburgh Centre, Edinburgh bioQuarter, The University of Edinburgh, Edinburgh EH16 4UU, United Kingdom; [g]Singapore Bioimaging Consortium (SBIC), Agency for Science, Technology and Research (A*STAR), 138667 Singapore; [h]Department of Life Sciences, Yeungnam University, Gyeongsan, Gyeongsangbuk-do 38541, South Korea; [i]Department of Physiology, National University of Singapore, 117597 Singapore; and [j]Department of Medicine, National University of Singapore, 117597 Singapore

Edited by Don W. Cleveland, University of California at San Diego, La Jolla, CA, and approved March 27, 2019 (received for review October 19, 2018)

White matter abnormalities are a nearly universal pathological feature of neurodegenerative disorders including Huntington disease (HD). A long-held assumption is that this white matter pathology is simply a secondary outcome of the progressive neuronal loss that manifests with advancing disease. Using a mouse model of HD, here we show that white matter and myelination abnormalities are an early disease feature appearing before the manifestation of any behavioral abnormalities or neuronal loss. We further show that selective inactivation of mutant huntingtin (mHTT) in the NG2+ oligodendrocyte progenitor cell population prevented myelin abnormalities and certain behavioral deficits in HD mice. Strikingly, the improvements in behavioral outcomes were seen despite the continued expression of mHTT in nonoligodendroglial cells including neurons, astrocytes, and microglia. Using RNA-seq and ChIP-seq analyses, we implicate a pathogenic mechanism that involves enhancement of polycomb repressive complex 2 (PRC2) activity by mHTT in the intrinsic oligodendroglial dysfunction and myelination deficits observed in HD. Our findings challenge the long-held dogma regarding the etiology of white matter pathology in HD and highlight the contribution of epigenetic mechanisms to the observed intrinsic oligodendroglial dysfunction. Our results further suggest that ameliorating white matter pathology and oligodendroglial dysfunction may be beneficial for HD.

Huntington disease | white matter | oligodendrocytes | myelination | PRC2

White matter (WM) structures are profoundly affected in nearly all neurodegenerative disorders. In Huntington disease (HD), morphometric and histological studies have shown myelin breakdown and loss of white matter volume in postmortem HD brains (1–3). Furthermore, structural magnetic resonance imaging (MRI) and diffusion tensor imaging have revealed volumetric atrophy and tract connectivity abnormalities in white matter regions in presymptomatic gene carriers and symptomatic patients with HD (4–6). Evidence of white matter abnormalities has also been observed in animal models of HD. Indeed, decreased expression in myelin basic protein (MBP) and thinner myelin sheaths was found in the BACHD mouse model of HD at a very early time point, weeks before the onset of behavioral phenotypes (7). In agreement with this, our laboratory has recently shown white matter microstructural abnormalities, thinner myelin sheaths, and a lower expression of myelin-related genes in the YAC128 mouse model of HD at a very early age (8, 9). Despite this prominence of white matter atrophy in HD, its etiology is not fully understood. It has long been assumed that white matter atrophy is secondary to neuronal loss. However, the appearance of white matter abnormalities very early in the disease course, indeed many years before neurological onset in patients (6, 10, 11) and before any neuronal loss in animal models of HD (7, 8, 12), suggests otherwise. Oligodendrocytes, the myelinating cells of the central nervous system (CNS), play a crucial role in maintaining axonal integrity and function. Deficits in oligodendrocytes or their precursors can lead to axonal pathology and neurodegeneration (13). Here, we hypothesize that intrinsic mutant huntingtin (mHTT)-mediated deficits in oligodendroglia contribute to myelination abnormalities and behavioral manifestations in HD. To test this hypothesis, we evaluated the impact of genetic reduction of mHTT in the oligodendrocyte progenitor cell (OPC) population specifically on myelination and behavioral phenotypes in HD mice.

Significance

Huntington disease (HD) is a progressive neurodegenerative disorder. While research efforts in HD have largely focused on understanding gray matter atrophy representing neuronal loss, there is clear evidence from human and animal studies that white matter structures, representing myelin-rich regions of the brain, are profoundly affected. Here, using an HD animal model, we show that myelin abnormalities appear before the manifestation of behavioral deficits or neuronal loss. Reduction of the mutant protein in oligodendrocytes, the myelinating cells of the central nervous system, prevented myelin abnormalities and certain behavioral deficits in HD mice. Our data implicate a glial pathogenic mechanism and suggest that directly targeting white matter pathology could be beneficial for HD. New therapeutic interventions targeting oligodendroglia should be considered.

Author contributions: C.F.B. and M.A.P. designed research; C.F.B., M.G.-M., N.S.C., N.A.R., R.T.Y.T., S.W., L.M.A., and H.-G.B. performed research; A.M.R., A.W., S.P., E.P., and M.R.H. contributed new reagents/analytic tools; C.F.B., N.S.C., S.R.L., N.H., S.J., and M.A.P. analyzed data; and C.F.B. and M.A.P. wrote the paper.

The authors declare no conflict of interest.

This article is a PNAS Direct Submission.

Data deposition: The RNA-seq and ChIP-seq sequencing data supporting the findings of this study have been deposited in the Sequence Read Archive under accession nos. SRP143632 and SRP159123, respectively.

[1]To whom correspondence should be addressed. Email: map@pouladilab.org.

This article contains supporting information online at www.pnas.org/lookup/suppl/doi:10.1073/pnas.1818042116/-/DCSupplemental.

Published online April 23, 2019.

Results

NG2Cre-Mediated Reduction of m*HTT* in Oligodendroglia. BACHD mice carry a full-length human mutant *HTT* gene modified to harbor a *loxP*-flanked exon 1 sequence (14). By crossing BACHD to NG2Cre mice that express the Cre recombinase in NG2+ OPCs (Fig. 1*A*), we were able to reduce mHTT expression specifically in oligodendroglia. Genomic PCR analysis showed successful excision of m*HTT* in the cortex of BACHDxNG2Cre (BN) mice (Fig. 1*B*). We further confirmed that m*HTT* mRNA levels in isolated NG2+ OPCs were reduced by ∼70% in BN mice (Fig. 1*C*).

OPC-Intrinsic Effects of mHTT Cause Myelin Deficits in HD Mice. To assess the impact of reducing m*HTT* expression specifically in OPCs on myelination deficits in HD, we used electron microscopy to visualize myelinated fibers in the corpus callosum, the largest white matter structure in the brain, at 12 mo of age (Fig. 1*D*). We examined g-ratios of myelinated axons, a measure of myelin sheath thickness calculated as the ratio of axon diameter (axon caliber) to myelinated fiber diameter. BACHD mice presented increased g-ratio compared with WT (Fig. 1*E*), indicating that their myelin sheaths were thinner. We found that selective reduction of m*HTT* in OPCs reversed this phenotype in BN mice (Fig. 1*F*). Indeed, the increased mean g-ratio in BACHD mice was rescued in BN mice, where it was comparable to WT mice (Fig. 1*G*). We also performed the same analysis at 1 mo of age (*SI Appendix*, Fig. S1*A*), where no significant differences in g-ratio were found among genotypes with one-way ANOVA. However, a binary *t* test of only WT and BACHD groups showed increased mean g-ratio in BACHD mice (*SI Appendix*, Fig. S1 *B* and *C*). This indicates that myelin sheaths in BACHD mice were thinner compared with WT mice as early as 1 mo of age, demonstrating that myelin abnormalities in HD are an early phenotype. Periodicity, a measure of myelin compaction calculated as the mean distance between two major dense lines, was also increased in BACHD mice, indicating less compact myelin compared with WT mice (*SI Appendix*, Fig. S1 *D* and *E*). Both abnormalities, mean g-ratio and periodicity, were rescued in BN mice (*SI Appendix*, Fig. S1 *B*–*E*). We next analyzed the number of myelinated axons in the corpus callosum (CC) and did not find any significant differences between the genotypes, suggesting no defects in the initiation of myelination (*SI Appendix*, Fig. S1*F*). To evaluate the functional impact of the WM abnormalities, we measured compound action potentials (CAPs) in the CC of BACHD brain slices at 14 mo of age. Quantification of the average stimulus–response revealed a modest decrease in the amplitude of the N1 component (myelinated axons), but not N2 (unmyelinated), in BACHD mice compared with WT mice, although the difference did not reach statistical significance (*SI Appendix*, Fig. S2*B*). BN mice showed a similar amplitude of the N1 component to WT mice (*SI Appendix*, Fig. S2 *A* and *B*). Furthermore, a modest but not significant decrease in the area of CAPs was detected on BACHD and BN in both N1 and N2 components, while duration of CAPs was comparable between the groups (*SI Appendix*, Fig. S2 *C* and *D*). The findings of the electron microscopy myelin sheath analyses clearly indicate that intrinsic oligodendroglial dysfunction mediated by mHTT contributes to structural myelination defects in HD. However, a conclusion of how this dysfunction impacts conduction velocity cannot be drawn due to the small sample size.

Behavioral Deficits in HD Mice Are Partly the Result of mHTT-Mediated Defects in Oligodendroglia. We next tested whether specific inactivation of m*HTT* in OPCs leads to improved motor and psychiatric-like behavioral phenotypes in BACHD mice. We evaluated mice at 2, 4, 6, 8, 10, and 12 mo of age using a battery of behavioral tests (Fig. 2*A*). BACHD mice exhibited motor deficits as early as 4 mo of age in the rotarod (latency to fall) and climbing (time climbing) tests, both reliable assays of motor impairment in BACHD mice (15). We found that BN mice showed improvements in the climbing test but not in rotarod training or performance (Fig. 2 *B*–*D*). The improvements in climbing performance of BN mice are most readily seen at 2–6 mo, with more comparable performance among the groups at later time points due to age-dependent decline in the WT and BN groups. BACHD mice also displayed psychiatric-like behavioral deficits, including anxiety-like behavior in the open-field (OF) test at 6 mo of age and depressive-like behavior in the Porsolt forced swim test (FST) at 12 mo of age, as shown previously (15). BN mice showed a modest improvement in the OF test, where the time spent in the center is not significantly different compared with WT mice, and a significant improvement in the FST (Fig. 2 *E* and *F*). To verify that this phenotype reflects psychiatric-like behavior rather than motor impairments, we tested the mice for swimming ability in a simple swim test. We showed that the ability to swim is comparable among genotypes (Fig. 2*G*).

To rule out the possibility that increased body weight may contribute to certain behavioral phenotypes, body weight was plotted against time climbing and time in center of OF at 6 mo of age and time immobile at 12 mo of age. Regression analysis revealed no correlation between body weight and climbing time (r2 = 0.10, $P = 0.24$ for WT; r2 = 0.01, $P = 0.72$ for NG2; r2 = 0.01, $P = 0.74$ for BACHD; r2 = 0.02, $P = 0.55$ for BN), between

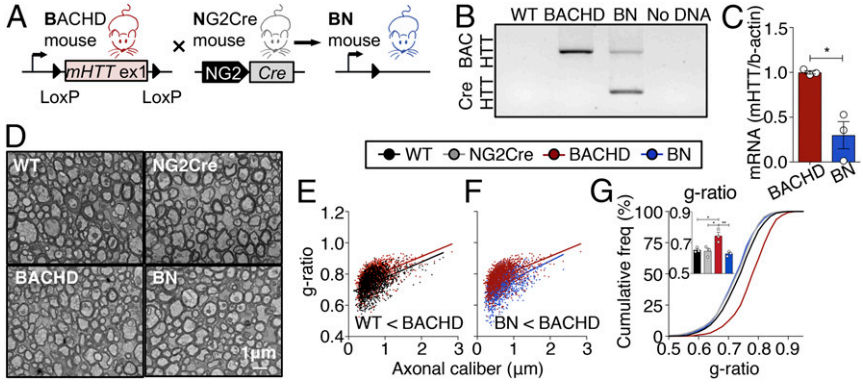

Fig. 1. OPC-intrinsic effects of mHTT cause myelination abnormalities in HD mice. (*A*) Schematic representation of Cre-mediated genetic reduction of mHTT expression in OPCs (NG2+ cells) in BACHD mice. (*B*) PCR analysis confirmed the excision of human mHTT exon 1 in the cortex of BN mice. (*C*) mHTT mRNA levels are reduced in purified OPCs in BN mice at P6–P7. $n = 3$/genotype ($P = 0.0100$, $t = 4.601$, df = 4). (*D*) EM images of myelinated axons in the CC at 12 mo of age. (Scale bar, 1 μm.) (*E*–*G*) Higher g-ratios (thinner myelin sheaths) in BACHD mice are rescued in BN mice. $n = 3$/genotype; ∼300 axons were quantified per animal. Data show means ± SEM; $*P < 0.05$, $**P < 0.01$; two-tailed Student's test in *C* and one-way ANOVA followed by Tukey's test in *G*.

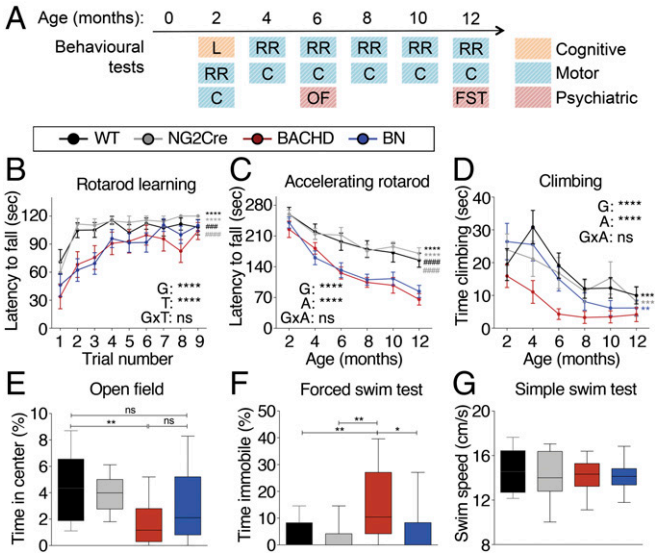

Fig. 2. Behavioral deficits in HD mice are partly the result of mHTT-mediated defects in oligodendroglia. (*A*) Overview of behavioral assessments. BACHD mice show cognitive deficits in the rotarod learning (*B*), motor deficits in the rotarod (*C*) and climbing (*D*) tests, anxiety-like behavior in the OF at 6 mo of age (*E*), and depressive-like behavior in the Porsolt FST at 12 mo of age (*F*). The ability to swim is comparable among genotypes at 12 mo of age (*G*). BN mice show a rescue in some of the behavioral phenotypes. $n = 12$–20 mixed gender/genotype. Data represent means ± SEM; ns, not significant; $^{*}P < 0.05$; $^{**}P < 0.01$; $^{***}P < 0.001$; $^{****}P < 0.0001$ (compared with BACHD); $^{\#\#\#}P < 0.001$; $^{\#\#\#\#}P < 0.0001$ (compare with BN). One-way ANOVA (*E*–*G*) or two-way ANOVA (*B*–*D*) followed by Tukey's multiple comparisons test were applied for all behavioral studies. A, age; G, genotype; T, trial.

body weight and time in center (r2 = 0.02, $P = 0.57$ for WT; r2 = 0.01, $P = 0.72$ for NG2; r2 = 0.09, $P = 0.31$ for BACHD; r2 = 0.12, $P = 0.13$ for BN), and between body weight and time immobile (r2 = 0.15, $P = 0.17$ for WT; r2 = 0.15, $P = 0.17$ for NG2; r2 = 0.004, $P = 0.82$ for BACHD; r2 = 0.04, $P = 0.39$ for BN), showing that increased body weight is not contributing to these behavioral phenotypes.

Therefore, selective inactivation of m*HTT* in OPCs improves certain aspects of motor and psychiatric-like deficits in BACHD mice, suggesting that mHTT-related effects in oligodendroglia contribute to the manifestation of some behavioral phenotypes in HD.

Absence of OPC-Intrinsic Effects of mHTT on Neuropathology and Oligodendrogenesis in HD Mice. We next addressed whether the specific inactivation of m*HTT* in OPCs can influence striatal atrophy in BACHD mice. We found that striatal volume was decreased in BACHD mice (*SI Appendix*, Fig. S3*B*) while forebrain weight was not significantly different among genotypes by one-way ANOVA. However, when a binary *t* test was used, BACHD mice showed a significant decrease in forebrain weight compared with WT (*SI Appendix*, Fig. S3*A*). Forebrain weight and striatal volume loss were not rescued in BN mice (*SI Appendix*, Fig. S3 *A* and *B*), suggesting that striatal pathology is not markedly impacted by mHTT-related oligodendroglial deficits.

Changes in the proliferation of NG2+ cells are observed in a wide variety of acute and chronic CNS conditions (16). To investigate whether oligodendroglia proliferation is altered in HD, we counted the number of cells that were positive for Olig2 (a transcription factor that marks the entire oligodendrocyte lineage), together with BrdU in the CC (*SI Appendix*, Fig. S3*C*). We also evaluated oligodendroglia density using Olig2, GST-pi (a marker of mature oligodendrocytes), and PDGFRα (an OPC marker) cell markers (*SI Appendix*, Fig. S3*D*). No changes were observed in oligodendroglia density or their proliferation in BACHD mice at 12 mo of age, suggesting that myelin pathology in BACHD mice is not associated with altered oligodendroglial proliferation or differentiation in adult mice. Also, we did not find any differences in the density or proliferation of oligodendroglia populations in the striatum and subventricular zone in BACHD mice compared with WT mice (*SI Appendix*, Fig. S3 *E*–*H*).

RNA-Seq Analysis Provides Insights into the Pathogenic Mechanisms. To gain insights into the pathogenic mechanisms underlying the oligodendrocyte dysfunction observed in HD mice, we performed RNA-seq analysis on the CC of WT, BACHD, and BN mice at 1 mo of age. We compared the gene expression profiles of the three genotypes and identified 360 significantly differentially expressed genes (DEGs) with a false discovery rate (FDR) of 10%. Hierarchical clustering of the gene expression from these DEGs revealed that the expression profile from BN mice was significantly closer to that of the WT mice than that of the BACHD mice ($P < 0.05$, Fig. 3*A* and Dataset S1).

We then compared gene expression profiles from BN and BACHD mice only and identified 449 DEGs (FDR < 10%, Fig. 3*B* and Dataset S1). Functional annotation of these DEGs revealed increases in the expression of key genes associated with myelination in BN mice versus synaptic transmission in BACHD mice (Fig. 3*C* and Dataset S2). A heatmap of representative myelin-related genes that were down-regulated in BACHD compared with WT mice and up-regulated in BN mice is shown in Fig. 3*D*. We also found that some myelin proteins such as Ermin, MBP, myelin-associated glycoprotein, and Septin-8 were indeed more highly expressed in BN versus BACHD mice (*SI Appendix*, Fig. S4 *A*–*D*). To examine whether certain DNA motifs were enriched in the DEGs, we applied a motif-discovery algorithm, HOMER (17). An Nkx2.2 consensus-binding motif, ACTTGGGAGG, was the top motif enriched among genes up-regulated in BN mice (Fig. 3*E* and *SI Appendix*, Table S1). Nkx2.2 plays a key role in the regulation of OPC differentiation (18) and is up-regulated during the OPC-to-oligodendrocyte transition (19). Interestingly, *Htt* is more highly expressed in OPCs and newly formed oligodendrocytes compared with more mature, myelinating oligodendrocytes (Fig. 3*F*) (20), suggesting the possibility of greater influence of the mutant HTT in OPCs and newly differentiated oligodendrocytes.

To further investigate the transcriptional changes identified, we performed transcription-factor/target-gene interactions analysis using ChEA, a database of ChIP-based studies (21). We found that DEGs between BACHD and BN mice were enriched for RE1 Regulation Transcription Factor (REST) and Polycomb Repressive Complex 2 (PRC2) binding sites (Fig. 3*G*). Dysregulation of REST has been implicated in HD, where, as a result of derepression by mutant HTT, it translocates from the cytoplasm to the nucleus in neurons leading to the repression of key neuronal genes such as *BDNF* (22). In OPCs, REST is required for the repression of neuronal properties and their development into oligodendrocytes (23). Here, however, the role of mHTT in REST dysregulation is not clear. PRC2 is a class of polycomb-group proteins thought to play a key role in the initiation of gene repression (24). Via EZH2, the catalytic subunit of the complex, PRC2 initiates repressive activity at target gene promoters by trimethylating histone H3 lysine 27 (H3K27me3). PRC2 plays a major role in lineage determination and cell-type specification, including oligodendroglia differentiation (25). PRC2 activity is indeed down-regulated at the earliest stages of neuron and astrocyte differentiation, while down-regulation of PRC2 activity in oligodendrocytes parallels their maturation (25). HTT is known to interact with and stimulate PRC2 activity in a polyglutamine length-dependent manner (26). Moreover, mHTT enhances PRC2 activity, increasing PRC2-specific histone H3K27 methylation. Here we propose a mechanism by which mHTT, enhancing PRC2 activity in oligodendroglia,

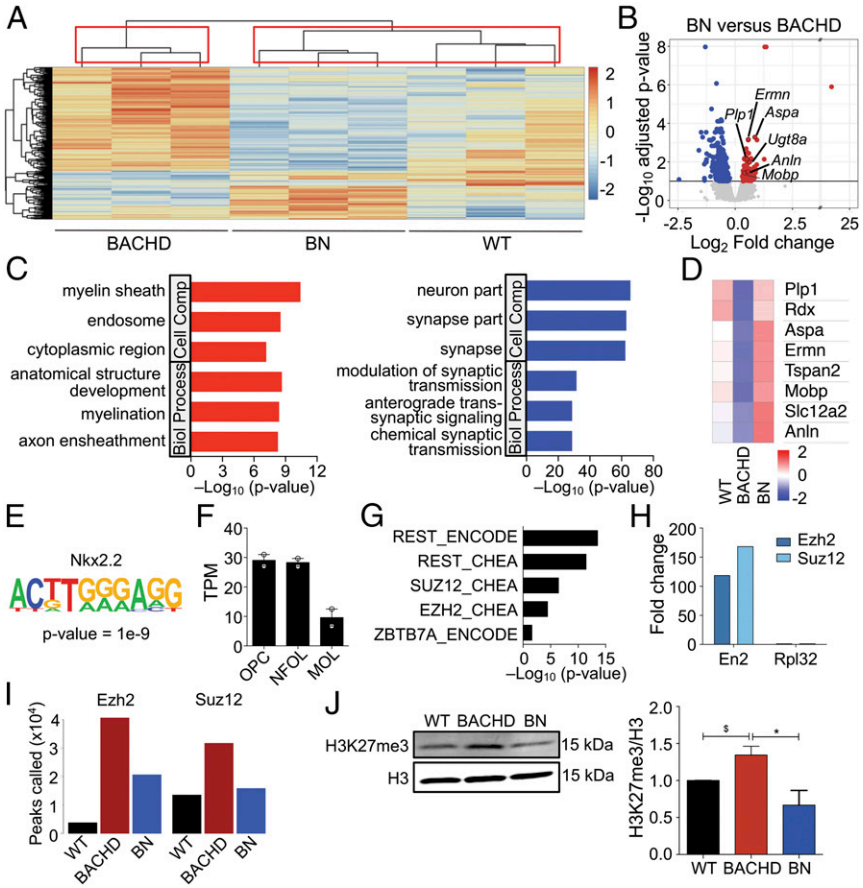

Fig. 3. Epigenetic dysregulation mediates mHTT effects on oligodendroglia. (*A*) Heatmap and hierarchal clustering of the significantly differentially expressed genes between WT ($n = 3$), BACHD ($n = 3$), and BN ($n = 3$) (360 genes, 10% FDR likelihood ratio test). Red indicates higher gene expression, and blue represents lower gene expression. Boxes indicate clusters of samples determined by 10,000 bootstraps. (*B*) Volcano plot showing the differentially expressed genes between BN ($n = 3$) and BACHD ($n = 3$) mouse corpus callosum. The significant up-regulated genes with respect to BN are indicated in red, while the significant down-regulated genes are indicated in blue (FDR < 10%). (*C*) Gene ontology analysis of significant DEGs between BACHD and BN mice. The top three significant terms (FDR < 5%) for up-regulated and down-regulated genes are shown. (*D*) Heat map shows mean gene expression levels of selected genes in WT, BACHD, and BN mice. (*E*) Nkx2.2 appears as the top motif enriched in up-regulated DEGs between BACHD and BN. (*F*) *Htt* gene expression (fragments per kilobase million) in different stages of oligodendroglial differentiation (data from ref. 20; $n = 2$ for each group, and bars indicate mean). MOL, myelinating oligodendrocytes; NFOL, newly formed oligodendrocytes; OPC, oligodendrocyte progenitor cells. (*G*) REST and PRC2-binding sites are enriched in DEGs between BACHD and BN. (*H*) ChIP-qPCR enrichment at the *En2* promoter in CC for EZH2 and SUZ12. Rpl32 was used as negative control. (*I*) Increased number of EZH2- and SUZ12-binding sites in the BACHD mice compared with WT is partially rescued in BN mice. (*J*) Immunoblot analysis of H3K27me3 in the CC of WT, BACHD, and BN mice. Values normalized to WT and presented as means ± SEM; $n = 3$ per genotype; $^{*}P < 0.05$ by one-way ANOVA with Tukey's post hoc test; $^{\$}P < 0.05$ by unpaired two-tailed *t* test.

leads to a delay in their maturation and results in myelination defects. To test the hypothesis of increased PRC2 activity in oligodendrocyte-enriched white matter regions as a result of mHTT, we performed chromatin immunoprecipitation followed by sequencing (ChIP-seq) analysis on the CC of WT, BACHD, and BN mice at 1 mo of age for EZH2 and SUZ12 (a subunit of PRC2).

Epigenetic Dysregulation Contributes to mHTT-Mediated Defects in Oligodendroglia. We first carried out ChIP-qPCR analysis, which showed high enrichment (EZH2 and SUZ12 occupancy) at the promoter of En2, a known target, compared with Rpl32 (negative control), in the CC of WT mice (Fig. 3*H*). ChIP-seq revealed an increased number of EZH2 and SUZ12 binding sites in BACHD compared with WT chromatin (Fig. 3*I*). We found that the increased EZH2 and SUZ12 peaks observed in BACHD mice are rescued in BN mice (Fig. 3*I*), implicating a role for excessive PRC2 activity in oligodendroglial dysfunction in HD. EZH2 and SUZ12 binding site peaks significantly overlapped under WT, BACHD, and BN conditions (*SI Appendix*, Fig. S5*A*). Enrichment analysis revealed that peaks with significantly higher binding of SUZ12 in BACHD compared with BN were enriched for processes including cerebellum development, the node of Ranvier, and a number of processes associated with differentiation and morphogenesis (*SI Appendix*, Fig. S5*B*). EZH2 peaks with higher binding in BACHD versus BN were enriched for similar processes including regulation of myelination and axonogenesis. *Plekhb1*, a gene highly expressed in myelin (27), was down-regulated in BACHD compared with BN (nominal *P* value < 0.05) and was found to only have an EZH2 peak close to its transcription start site (TSS) in BACHD and not in WT or BN (*SI Appendix*, Fig. S5*D*).

We compared the set of genes the promoters (±5 kb from the TSS) of which were were differentially bound by EZH2 between BN and BACHD (Dataset S3) with the set of genes identified as differentially expressed between BN and BACHD. We found that the set of DEGs was significantly enriched for differential EZH2 binding in their promoters (11% of DEGs, $P = 0.001$, χ^2 test). These differentially bound DEGs included genes involved in myelination such as Semaphorin-4D (Sema4d) (28). In contrast, the set of DEGs between BN and WT showed no enrichment for differential binding of EZH2 (7% of DEGs, $P = 0.40$, χ^2 test). Differential binding of SUZ12 in the promoter regions (Dataset S3) did not show an enrichment in the set of DEGs. Finally, we assessed the levels of H3K27me3 in the CC of WT, BACHD, and BN mice as a global measure of PRC2 activity. Consistent with the ChIP-seq results, we found that the elevated levels of H3K27me3 in BACHD mice are rescued in BN mice (Fig. 3*J*). These results implicate differences in the binding and activity of PRC2, driven by mHTT, in the dysregulation of key genes involved in oligodendrocyte myelination.

Discussion

In this study, we provide strong evidence for intrinsic mutant HTT-mediated defects in oligodendroglia leading to myelination deficits and behavioral abnormalities in HD and contributing to the overall pathology of HD. Consistent with previous studies of animal models of HD (7, 8), we show that BACHD mice exhibit thinner myelin and decreased myelin compaction as early as 1 mo of age, suggesting that myelin abnormalities in HD are an early phenotype. The appearance of white matter abnormalities early in the disease course is in agreement with clinical studies, where it appears many years before neurological onset in patients (6, 10). We show that these early phenotypes worsen with age, with greater myelin thinning in BACHD mice at 12 mo old, indicating that myelin structure deteriorates with disease progression, in

line with the worsening of WM pathology in subjects with HD as the disease progresses (10). While myelination abnormalities in HD have long been considered to be a secondary effect of axonal degeneration, here we show that they are primarily driven by intrinsic oligodendroglial dysfunction in early stages of disease and are rescuable by inactivating m*HTT* in oligodendroglia.

WM abnormalities have been linked to neuropsychiatric disorders, including HD (29) and major depression (30–32), where disconnection of WM regions including the CC has been reported. In addition, loss of NG2-expressing glial cells has been shown to trigger depressive-like behaviors in mice (33). Motor and cognitive abnormalities have also been associated with changes in white matter structure in several disorders including HD (34, 35). Our observations of improved psychiatric-like phenotypes, such as a rescue in the FST, and motor function that accompanied the improvements in myelination (e.g., rescue of increased callosal g-ratios) in BN mice support this link between WM abnormalities and neurological deficits.

While inactivation of m*HTT* in oligodendroglia rescues myelin deficits and ameliorates certain aspects of behavioral phenotypes, it is not sufficient alone to improve striatal neuropathology in HD mice. This lack of rescue of striatal atrophy may not be entirely surprising given that mutant HTT remains expressed in neurons and other glial cell types and thus continues to exert its detrimental effects on the function and survival of striatal neurons. Moreover, medium spiny neurons, which are the major neuronal population in the striatum and the most vulnerable neurons in HD (36), have very short projections and are mostly unmyelinated and thus may not benefit directly from improved oligodendroglial function.

Two mechanisms that underlie myelination deficits in HD have been proposed: abnormal cholesterol metabolism (7) and myelin regulator factor (MYRF) dysregulation by its abnormal association with mHTT (37). MYRF regulates oligodendrocyte maturation and is essential for proper myelination (38). Reduction of MYRF transcriptional activity has been associated with oligodendroglial dysfunction and myelin impairment in HD (37). Decreased cholesterol biosynthesis has been linked to impaired activity of peroxisome-proliferator–activated receptor gamma coactivator 1 alpha (PGC1α) in HD (7). Here we implicate enhancement of PRC2 activity by mHTT in intrinsic oligodendroglial dysfunction and myelination deficits in HD, highlighting the contribution of epigenetic mechanisms to HD white matter pathology. Oligodendroglia development is regulated by a dynamic interaction between genetic and epigenetic factors. EZH2, a component of PRC2, is a histone methyltransferase that, through the methylation of lysine 27 on histone H3 (H3K27), plays a crucial role in oligodendroglia lineage determination (25). A number of compounds have been developed to dampen PRC2 function by inhibiting the enzymatic activity of EZH2 (39). Targeting PRC2 activity with such EZH2 antagonists would help address whether reducing PRC2 activity could lead to improvements in myelination deficits in HD. Given its broad activity and ubiquitous expression, however, it is doubtful that targeting general PRC2 activity would be a viable therapeutic strategy for HD. Nonetheless, efforts to establish the basis of interaction between mutant HTT and PRC2 may reveal novel strategies for moderation of HTT's interaction with PRC2 and normalization of its activity. Such targeted mutant HTT-specific approaches have the potential to provide therapeutic benefit while at the same time minimizing undesirable side effects.

While not validated in the current study, our analysis also highlights a potential role for dysregulation of Nkx2.2 target genes in the myelination deficits in HD. Of note, a recent human pluripotent stem-cell–based study has provided evidence that transcriptional targets of Nkx2.2 are down-regulated in HD oligodendroglia compared with control (40). These studies together with our findings indicate a role for deficits in multiple oligodendroglia processes as primary contributors to myelination abnormalities in HD. However, the degree of interdependence and the relative contribution of the different pathways identified to WM pathology in HD remains to be determined.

Emerging evidence suggests that neurodevelopment may be altered in HD (41), including several aspects related to oligodendroglia. For example, mice expressing reduced levels of Htt throughout development exhibit OPC maturation abnormalities and white matter tract impairments (42). OPCs isolated from neonatal HD mouse brains and derivative oligodendrocytes show deficits in the levels of myelin-related genes (8). Mouse HD embryonic stem cells show altered oligodendrogenesis upon neural induction (43), and OPCs derived from human HD embryonic stem cells show dysregulation in myelin-related transcriptional profiles as well as altered myelination properties (40). Our observations of early postnatal deficits in myelination (e.g., as early as 1 mo of age) are in line with the possibility that the myelination deficits in HD originate during development and persist with age. An outstanding question that remains, particularly in the context of the HTT-lowering therapeutic efforts currently underway, is whether inactivating mutant HTT in mature oligodendrocytes in adulthood would rescue the myelination abnormalities and associated neurological deficits.

In addition to oligodendroglia in the CNS, NG2 is also expressed by Schwann cells in the peripheral nervous system (44). Although in the few studies that have examined Schwann cells in HD, these cells were found to be unaffected (45), their possible role in the current study was not evaluated. Future studies to investigate possible Schwann cell pathology and any relationship to disease manifestations in HD should be considered.

A better understanding of the mechanisms underlying myelination deficits could shed light on new therapeutic approaches for HD. Strategies for intervention should be expanded from the current neuro-centric focus of most therapeutic efforts to include oligodendroglial targets. Indeed, our data suggest that directly targeting white matter pathology could be beneficial for HD.

Materials and Methods

Animals. Mice were maintained under standard conditions and all animal procedures were performed with the approval of the Institutional Animal Care and Use Committee (IACUC #151067) at Biological Resource Centre (BRC), A*STAR, and in accordance with their approved guidelines. BACHD specific-pathogen-free (SPF) mice (stock no. 008197; JAX) were maintained on the FVB/N background. NG2-Cre SPF mice (stock no. 008533; JAX) were backcrossed onto the FVB/N background and then bred to generate BACHD-NG2Cre mice. Cre-excision validation was performed by PCR on genomic DNA using primers listed in *SI Appendix*, Table S2. For details, see *SI Appendix*.

PCR for Cre-Excision Validation. Genomic DNA was extracted from dissected frozen mouse cortex at 1 mo of age using the DNeasy Tissue kit (Qiagen). To visualize the successful deletion of HTT exon 1 in BACHDxNG2Cre mice, the PCR products were run on a 1% agarose gel with SYBER Safe DNA gel stain (Invitrogen). The primers flanking the loxP sites of HTT exon 1 in the BACHD mice are summarized in *SI Appendix*, Table S2.

Real-Time Quantitative PCR. Brains from postnatal day (P) 6 to P7 pups were collected and dissociated with the Neural Tissue Dissociation Kit (Miltenyi Biotec). A pure population of NG2+ OPCs was isolated using anti-AN2 magnetic microbeads (Miletenyi Biotec) through magnetic-activated cell sorting separation. For details, see *SI Appendix*.

Transmission Electron Microscopy. Mice were transcardially perfused with 2.5% glutaraldehyde and 2.5% paraformaldehyde (PFA) in PBS before postfixing the brains overnight at 4 °C in the same buffer. Brains were subsequently washed in PBS and transferred in 5% sucrose plus 0.08% NaN3 in PBS. For details, see *SI Appendix*.

Corpora Callosa Slice Preparation and Electrophysiology. Fourteen-month-old 1 female mice were used for this experiment. Animals' brains were carefully dissected after cervical dislocation and placed in oxygenated (95% O2 + 5% CO_2) ice-cold sucrose artificial cerebrospinal fluid cutting solution. For details and for the CAP recording, see *SI Appendix*.

Behavioral Test of Affective Function. All of the behavioral tests were performed during the dark phase of the reverse light/dark cycle. One independent cohort was used with $n = 12–20$ mixed gender per genotype (body weight in grams ± SD: 20.56 ± 3.15 in WT, 20.28 ± 3.54 in NG2Cre, 24.16 ± 3.47 in BACHD, and 19.99 ± 3.23 in BN at 6 wk). For details, see *SI Appendix*.

Immunohistochemistry and Stereological Measurements. For immunohistochemistry and stereological measurements, one independent cohort was used with $n = 13–18$ per genotype. For cell proliferation studies, 200 mg/kg of BrdU (B9285; Sigma) was injected intraperitoneally for 3 d at 12-h intervals before transcardial perfusion with 4% PFA and brain extraction. For details and antibodies used, see *SI Appendix*.

Protein Analysis. Protein lysate of CC from male mice were prepared using RIPA buffer (Sigma-Aldrich) with 1 mM PMSF (Sigma-Aldrich), 5 μm Z-VAD (Promega), 1 mM NaVan (Sigma-Aldrich), and 1× Complete Protease Inhibitor Mixture tablets (Roche). For details and antibodies used, see *SI Appendix*.

RNA-Seq and ChIP-Seq Analysis. RNA was extracted from mouse CC (WT, $n = 3$; BACHD, $n = 3$; BN, $n = 3$) using TRIzol (Life Technologies) and subsequently a RNeasy plus mini kit (Qiagen) according to the manufacturer's instructions. For ChIP-seq analysis, mouse CC tissues were microdissected and pooled from 12 mice per sample at 1 mo of age. For details of RNA-seq and ChIP-seq analyses (46), see *SI Appendix*.

ACKNOWLEDGMENTS. We thank members of the M.A.P. laboratory for helpful discussions and comments. C.F.B. is supported by a Singapore International Graduate Award from the Agency for Science, Technology and Research (A*STAR). M.A.P. is supported by grants from A*STAR and the National University of Singapore.

1. de la Monte SM, Vonsattel JP, Richardson EP, Jr (1988) Morphometric demonstration of atrophic changes in the cerebral cortex, white matter, and neostriatum in Huntington's disease. *J Neuropathol Exp Neurol* 47:516–525.
2. Mann DMA, Oliver R, Snowden JS (1993) The topographic distribution of brain atrophy in Huntington's disease and progressive supranuclear palsy. *Acta Neuropathol* 85:553–559.
3. Bartzokis G, et al. (2007) Myelin breakdown and iron changes in Huntington's disease: Pathogenesis and treatment implications. *Neurochem Res* 32:1655–1664.
4. Reading SAJ, et al. (2005) Regional white matter change in pre-symptomatic Huntington's disease: A diffusion tensor imaging study. *Psychiatry Res* 140:55–62.
5. Rosas HD, et al. (2006) Diffusion tensor imaging in presymptomatic and early Huntington's disease: Selective white matter pathology and its relationship to clinical measures. *Mov Disord* 21:1317–1325.
6. Rosas HD, et al. (2018) Complex spatial and temporally defined myelin and axonal degeneration in Huntington disease. *Neuroimage Clin* 20:236–242.
7. Xiang Z, et al. (2011) Peroxisome-proliferator-activated receptor gamma coactivator 1 α contributes to dysmyelination in experimental models of Huntington's disease. *J Neurosci* 31:9544–9553.
8. Teo RTY, et al. (2016) Structural and molecular myelination deficits occur prior to neuronal loss in the YAC128 and BACHD models of Huntington disease. *Hum Mol Genet* 25:2621–2632.
9. Garcia-Miralles M, et al. (2018) Laquinimod treatment improves myelination deficits at the transcriptional and ultrastructural levels in the YAC128 mouse model of Huntington disease. *Mol Neurobiol*, 10.1007/s12035-018-1393-1.
10. Tabrizi SJ, et al.; TRACK-HD investigators (2009) Biological and clinical manifestations of Huntington's disease in the longitudinal TRACK-HD study: Cross-sectional analysis of baseline data. *Lancet Neurol* 8:791–801.
11. Paulsen JS, et al.; Predict-HD Investigators and Coordinators of the Huntington Study Group (2008) Detection of Huntington's disease decades before diagnosis: The predict-HD study. *J Neurol Neurosurg Psychiatry* 79:874–880.
12. Carroll JB, et al. (2011) Natural history of disease in the YAC128 mouse reveals a discrete signature of pathology in Huntington disease. *Neurobiol Dis* 43:257–265.
13. Nave K-A (2010) Myelination and support of axonal integrity by glia. *Nature* 468: 244–252.
14. Gray M, et al. (2008) Full-length human mutant huntingtin with a stable polyglutamine repeat can elicit progressive and selective neuropathogenesis in BACHD mice. *J Neurosci* 28:6182–6195.
15. Pouladi MA, et al. (2012) Marked differences in neurochemistry and aggregates despite similar behavioural and neuropathological features of Huntington disease in the full-length BACHD and YAC128 mice. *Hum Mol Genet* 21:2219–2232.
16. Levine JM, Reynolds R, Fawcett JW (2001) The oligodendrocyte precursor cell in health and disease. *Trends Neurosci* 24:39–47.
17. Heinz S, et al. (2010) Simple combinations of lineage-determining transcription factors prime cis-regulatory elements required for macrophage and B cell identities. *Mol Cell* 38:576–589.
18. Qi Y, et al. (2001) Control of oligodendrocyte differentiation by the Nkx2.2 homeodomain transcription factor. *Development* 128:2723–2733.
19. Hu BY, Du ZW, Li XJ, Ayala M, Zhang SC (2009) Human oligodendrocytes from embryonic stem cells: Conserved SHH signaling networks and divergent FGF effects. *Development* 136:1443–1452.
20. Zhang Y, et al. (2014) An RNA-sequencing transcriptome and splicing database of glia, neurons, and vascular cells of the cerebral cortex. *J Neurosci* 34:11929–11947.
21. Lachmann A, et al. (2010) ChEA: Transcription factor regulation inferred from integrating genome-wide ChIP-X experiments. *Bioinformatics* 26:2438–2444.
22. Zuccato C, et al. (2003) Huntingtin interacts with REST/NRSF to modulate the transcription of NRSE-controlled neuronal genes. *Nat Genet* 35:76–83.
23. Dewald LE, Rodriguez JP, Levine JM (2011) The RE1 binding protein REST regulates oligodendrocyte differentiation. *J Neurosci* 31:3470–3483.
24. Margueron R, Reinberg D (2011) The Polycomb complex PRC2 and its mark in life. *Nature* 469:343–349.
25. Sher F, et al. (2008) Differentiation of neural stem cells into oligodendrocytes: Involvement of the polycomb group protein Ezh2. *Stem Cells* 26:2875–2883.
26. Seong I, et al. (2010) Huntingtin facilitates polycomb repressive complex 2. *Hum Mol Genet* 19:573–583.
27. Thakurela S, et al. (2016) The transcriptome of mouse central nervous system myelin. *Sci Rep* 6:25828.
28. Moreau-Fauvarque C, et al. (2003) The transmembrane semaphorin Sema4D/CD100, an inhibitor of axonal growth, is expressed on oligodendrocytes and upregulated after CNS lesion. *J Neurosci* 23:9229–9239.
29. Sprengelmeyer R, et al. (2014) The neuroanatomy of subthreshold depressive symptoms in Huntington's disease: A combined diffusion tensor imaging (DTI) and voxel-based morphometry (VBM) study. *Psychol Med* 44:1867–1878.
30. Edgar N, Sibille E (2012) A putative functional role for oligodendrocytes in mood regulation. *Transl Psychiatry* 2:e109.
31. Nave K-A, Ehrenreich H (2014) Myelination and oligodendrocyte functions in psychiatric diseases. *JAMA Psychiatry* 71:582–584.
32. Shen X, et al. (2017) Subcortical volume and white matter integrity abnormalities in major depressive disorder: Findings from UK Biobank imaging data. *Sci Rep* 7:5547.
33. Birey F, et al. (2015) Genetic and stress-induced loss of NG2 glia triggers emergence of depressive-like behaviors through reduced secretion of FGF2. *Neuron* 88:941–956.
34. Bohnen NI, Albin RL (2011) White matter lesions in Parkinson disease. *Nat Rev Neurol* 7:229–236.
35. Poudel GR, et al. (2014) White matter connectivity reflects clinical and cognitive status in Huntington's disease. *Neurobiol Dis* 65:180–187.
36. Tepper JM, Bolam JP (2004) Functional diversity and specificity of neostriatal interneurons. *Curr Opin Neurobiol* 14:685–692.
37. Huang B, et al. (2015) Mutant huntingtin downregulates myelin regulatory factor-mediated myelin gene expression and affects mature oligodendrocytes. *Neuron* 85: 1212–1226.
38. Koenning M, et al. (2012) Myelin gene regulatory factor is required for maintenance of myelin and mature oligodendrocyte identity in the adult CNS. *J Neurosci* 32: 12528–12542.
39. Kim KH, Roberts CWM (2016) Targeting EZH2 in cancer. *Nat Med* 22:128–134.
40. Osipovitch M, et al. (2019) Human ESC-derived chimeric mouse models of Huntington's disease reveal cell-intrinsic defects in glial progenitor cell differentiation. *Cell Stem Cell* 24:107–122.e7.
41. Humbert S (2010) Is Huntington disease a developmental disorder? *EMBO Rep* 11:899.
42. Arteaga-Bracho EE, et al. (2016) Postnatal and adult consequences of loss of huntingtin during development: Implications for Huntington's disease. *Neurobiol Dis* 96: 144–155.
43. Nguyen GD, Gokhan S, Molero AE, Mehler MF (2013) Selective roles of normal and mutant huntingtin in neural induction and early neurogenesis. *PLoS One* 8:e64368.
44. Schneider S, et al. (2001) The AN2 protein is a novel marker for the Schwann cell lineage expressed by immature and nonmyelinating Schwann cells. *J Neurosci* 21: 920–933.
45. Ribchester RR, et al. (2004) Progressive abnormalities in skeletal muscle and neuromuscular junctions of transgenic mice expressing the Huntington's disease mutation. *Eur J Neurosci* 20:3092–3114.
46. Leinonen R, Sugawara H, Shumway M (2011) The sequence read archive. *Nucleic Acids Res* 39:D19–D21.